

SLAC-PUB-7401  
MIT-LNS-97-237

January 1997

**THREE-JET EVENT ORIENTATION  
IN  $e^+e^-$  ANNIHILATION:  
NEW TESTS OF THE STANDARD MODEL\***

**P.N. Burrows\*\***

*Stanford Linear Accelerator Center  
Stanford University, Stanford, CA 94309, USA*

burrows@slac.stanford.edu

**P. Osland**

*Department of Physics, University of Bergen  
Allégt. 55, N-5007 Bergen, Norway*

per.osland@fi.uib.no

**Abstract**

We discuss the orientation of  $e^+e^- \rightarrow q\bar{q}g$  events in terms of the polar and azimuthal angles of the event plane w.r.t. the electron beam direction. We define an asymmetry of the azimuthal-angle distribution which, along with the left-right forward-backward polar-angle asymmetry, is sensitive to parity-violating effects in three-jet events; these have yet to be explored experimentally. We have evaluated these observables at  $O(\alpha_s)$  in perturbative QCD and present their dependence on longitudinal beam polarisation and c.m. energy. We also define a moments analysis in terms of the orientation angles that allows a new and more detailed test of QCD by isolating the six independent helicity cross-sections.

*Submitted to Physics Letters B*

\* Work supported by Department of Energy contracts DE-FC02-94ER40818 (MIT) and DE-AC03-76SF00515 (SLAC).

\*\* Permanent address: Lab. for Nuclear Science, M.I.T., Cambridge, MA 02139, USA.

## 1. Introduction

In  $e^+e^-$  annihilation, events containing three distinct jets of hadrons were first observed many years ago at the PETRA storage ring [1]. Such events were interpreted in terms of the fundamental process  $e^+e^- \rightarrow q\bar{q}g$  (Fig. 1), providing direct evidence for the existence of the gluon, the vector boson of the theory of strong interactions, Quantum Chromodynamics (QCD) [2]. A large number of subsequent studies of the properties of such events [3] has verified this interpretation.

Here we consider the orientation of the  $q\bar{q}g$  plane or ‘event plane’ in terms of the angles  $\theta$  and  $\chi$  (Fig. 2), where  $\theta$  is the polar angle of the quark direction with respect to the electron beam, and  $\chi$  is the azimuthal orientation angle of the event plane with respect to the quark-electron plane, such that:

$$\cos \chi = \frac{\vec{q} \times \vec{g}}{|\vec{q} \times \vec{g}|} \cdot \frac{\vec{q} \times \vec{e}^-}{|\vec{q} \times \vec{e}^-|}. \quad (1)$$

The polar angle can also be defined in two-jet events of the type  $e^+e^- \rightarrow q\bar{q}$ , in which case the distribution in  $\theta$  is determined in the electroweak theory [4], and displays a c.m. energy-dependent forward-backward asymmetry which has been observed in many experiments [5], [6]. For  $e^+e^-$  annihilation at the  $Z^0$  resonance, the polar-angle asymmetry is large only if one, or both, of the beams is longitudinally polarised, as at SLC/SLD [7]. The azimuthal angle  $\chi$  is, of course, undefined in  $q\bar{q}$  events, but in  $q\bar{q}g$  events, as we shall show, it also displays an asymmetry which can be large at the  $Z^0$  resonance in the case of highly polarised electrons. This azimuthal-angle distribution has not yet been investigated experimentally.

We review (Section 2) the fully-differential cross-section for three-jet production in  $e^+e^-$  annihilation, and present (Section 3) the polar- and azimuthal-angle distributions, illustrating their dependence on the longitudinal electron beam polarisation and the c.m. energy. In Section 4 we consider asymmetries of these angular distributions, which provide a currently unexplored search ground for anomalous parity-violating effects in  $q\bar{q}g$  events. In Section 5 we define moments of the cross-section in terms of  $\cos \theta$  and  $\cos \chi$ , which would allow one to make a more detailed test of QCD by determining the six independent helicity cross-sections, which have not yet been directly explored experimentally. In Section 6 we discuss more inclusive cases in which the requirement of

quark and antiquark jet identification is relaxed, and in Section 7 we present a summary and concluding remarks.

## 2. Review of the $e^+e^- \rightarrow q\bar{q}g$ Differential Cross-Section

Firstly, we give a brief review of the differential cross-section for three-jet production in  $e^+e^-$  annihilation at c.m. energy  $\sqrt{s}$ , assuming massless partons. Let  $\vec{q}$ ,  $\vec{\bar{q}}$ , and  $\vec{g}$  denote the quark, antiquark and gluon momenta respectively, and  $x$ ,  $\bar{x}$  and  $x_g$  be the scaled energies:

$$|\vec{q}| = x\sqrt{s}, \quad |\vec{\bar{q}}| = \bar{x}\sqrt{s}, \quad |\vec{g}| = x_g\sqrt{s}, \quad (2)$$

with  $x + \bar{x} + x_g = 2$ . Allowing for longitudinal beam polarisation<sup>#1</sup>, the fully-differential three-jet cross-section can then be expressed as [8]:

$$\begin{aligned} 2\pi \frac{d^4\sigma}{d(\cos\theta)d\chi dx d\bar{x}} = & \left[ \frac{3}{8}(1 + \cos^2\theta) \frac{d^2\sigma_U}{dx d\bar{x}} + \frac{3}{4}\sin^2\theta \frac{d^2\sigma_L}{dx d\bar{x}} \right. \\ & + \frac{3}{4}\sin^2\theta \cos 2\chi \frac{d^2\sigma_T}{dx d\bar{x}} + \frac{3}{2\sqrt{2}}\sin 2\theta \cos \chi \frac{d^2\sigma_I}{dx d\bar{x}} \left. \right] h_f^{(1)}(s) \\ & + \left[ \frac{3}{4}\cos\theta \frac{d^2\sigma_P}{dx d\bar{x}} - \frac{3}{\sqrt{2}}\sin\theta \cos \chi \frac{d^2\sigma_A}{dx d\bar{x}} \right] h_f^{(2)}(s), \end{aligned} \quad (3)$$

where at lowest order in the electroweak theory the dependences on flavour and beam polarisation are given by the functions:

$$\begin{aligned} h_f^{(1)}(s) = & Q_f^2 \Xi - 2Q_f \text{Re } f(s)(v\Xi - a\xi)v_f \\ & + |f(s)|^2[(v^2 + a^2)\Xi - 2va\xi](v_f^2 + a_f^2), \end{aligned} \quad (4)$$

$$\begin{aligned} h_f^{(2)}(s) = & -2Q_f \text{Re } f(s)(a\Xi - v\xi)a_f \\ & + |f(s)|^2[-(v^2 + a^2)\xi + 2va\Xi]2v_fa_f, \end{aligned} \quad (5)$$

with

$$f(s) = \frac{1}{4\sin^2 2\theta_W} \frac{s}{s - M_Z^2 + iM_Z\Gamma_Z^{\text{tot}}}, \quad (6)$$

where  $Q_f$  is the charge of quark flavour  $f$ ;  $v$ ,  $a$  ( $v_f$ ,  $a_f$ ) are the vector and axial vector couplings of the  $Z^0$  to the electron (quark of flavour  $f$ ), respectively,

$$\Xi = 1 - P_-^\parallel P_+^\parallel, \quad \xi = P_-^\parallel - P_+^\parallel, \quad (7)$$

---

<sup>#1</sup> Expressions for the general case of arbitrarily polarised beams are given in [8].

and  $P_-^\parallel$  ( $P_+^\parallel$ ) is the longitudinal polarisation of the electron (positron) beam.

Several important points concerning eq. (3) should be noted. The cross-section can be written as a sum of 6 terms, each of which may be factorised into three contributions: the first factor is a simple trigonometric function of the polar and azimuthal orientation angles  $\theta$  and  $\chi$ , and the second,  $d^2\sigma_i/dxd\bar{x}$  ( $i=U, L, T, I, P, A$ ), is a function of the parton momentum fractions; these are determined by QCD and kinematics; the third factor,  $h_f^{(1,2)}(s)$ , is a function containing the dependence on the fermion electroweak couplings. Hence, in each term there is factorisation both between the dynamical contributions of the QCD and electroweak sectors of the Standard Model and between the orientation of the event plane and the relative orientation of the jets within the plane. We exploit this property later by defining moments in terms of  $\cos\theta$  and  $\cos\chi$  in order to isolate the different terms. The  $\sigma_i$  are often referred to in the literature as *helicity cross-sections*<sup>#2</sup>, and the form of eq. (3), with six terms, each containing one of the six independent helicity cross-sections, has been shown [10] to be valid for massless partons up to  $O(\alpha_s^2)$  in perturbative QCD.

At  $O(\alpha_s)$  in perturbative QCD [8], [11]:

$$\frac{d^2\sigma_i}{dxd\bar{x}} = \frac{\tilde{\sigma}}{(1-x)(1-\bar{x})} F_i, \quad (8)$$

where

$$\tilde{\sigma} = \frac{4\pi\alpha^2\alpha_s(s)}{3\pi s}. \quad (9)$$

For the coordinate system of Fig. 2 one has [8]:

$$\begin{aligned} F_U &= 2x^2 + \bar{x}^2(1 + \bar{c}^2), & F_L &= \bar{x}^2\bar{s}^2, \\ F_T &= \frac{1}{2}F_L, & F_I &= 2^{-1/2}\bar{x}^2\bar{c}\bar{s}, \\ F_A &= 2^{-1/2}\bar{x}^2\bar{s}, & F_P &= 2(x^2 - \bar{x}^2\bar{c}), \end{aligned} \quad (10)$$

where  $\bar{c} = \cos(\psi_{q\bar{q}})$  and  $\bar{s} = \sin(\psi_{q\bar{q}})$ , with  $\psi_{q\bar{q}}$  the angle between the quark and antiquark momenta. Since the quark and antiquark tend to have a small acollinearity angle,  $F_L$ ,  $F_T$ ,  $F_I$  and  $F_A$  will typically be small compared with  $F_U$  and  $F_P$ .

---

<sup>#2</sup> Helicity cross sections have also been discussed in the context of single-particle inclusive fragmentation functions [9].

### 3. Polar- and Azimuthal-Angle Distributions

We now discuss the singly-differential cross-sections in terms of  $\cos\theta$  or  $\chi$ . Consider integrating eq. (3) first over  $x$  and  $\bar{x}$ , with the integration domain given by a standard jet resolution criterion  $y_c$ <sup>#3</sup> and using the notation:

$$\hat{\sigma}_i \equiv \int_{y_c} dx \int d\bar{x} \frac{d^2\sigma_i}{dx d\bar{x}}. \quad (11)$$

Integrating over  $\chi$  we then obtain:

$$\frac{d\sigma}{d(\cos\theta)} = \left( \frac{3}{8}(1 + \cos^2\theta) \hat{\sigma}_U + \frac{3}{4} \sin^2\theta \hat{\sigma}_L \right) h_f^{(1)}(s) + \frac{3}{4} \cos\theta \hat{\sigma}_P h_f^{(2)}(s), \quad (12)$$

where the term containing  $\hat{\sigma}_P$  represents the well-known quark forward-backward asymmetry resulting from parity violation in the weak interaction, but for the three-jet case. Similarly, by integrating over  $\cos\theta$  we obtain:

$$2\pi \frac{d\sigma}{d\chi} = (\hat{\sigma}_U + \hat{\sigma}_L + \cos 2\chi \hat{\sigma}_T) h_f^{(1)}(s) - \frac{3\pi}{2\sqrt{2}} \cos\chi \hat{\sigma}_A h_f^{(2)}(s), \quad (13)$$

where the term containing  $\hat{\sigma}_A$  represents an azimuthal, parity-odd asymmetry analogous to the last term in eq. (12) but owing its existence to the radiation of the gluon.

For the case of longitudinally-polarised electrons and unpolarised positrons the dependences of these singly-differential distributions on the beam polarisation and c.m. energy are illustrated in Figs. 3(a,b) and 4(a,b) respectively. We calculated the  $\sigma_i$  at  $O(\alpha_s)$  as in Ref. [8]. Fig. 3a shows the distribution in  $\cos\theta$  at  $\sqrt{s} = M_Z$  for down-type quarks,  $y_c = 0.02$  and electron longitudinal polarisation  $p = +1, 0$  and  $-1$ .<sup>#4</sup> The current SLC/SLD case of  $p = \pm 0.77$  [13] is also indicated. The quark polar-angle forward-backward asymmetry is large for high beam polarisation, and its sign changes with the sign of the polarisation. The less familiar azimuthal-angle distribution is shown in Fig. 3b for the same cases as in Fig. 3a; the distribution is symmetric about  $\chi = \pi$ . The phase change of the  $\chi$  distribution when the beam polarisation sign is changed is a

---

<sup>#3</sup> Any of the six infra-red- and collinear-safe jet-definition algorithms ‘E’, ‘E0’, ‘P’, ‘P0’, ‘D’ and ‘G’ [12] could be used. We have used the ‘E’ procedure which, at  $O(\alpha_s)$ , gives identical results to the ‘E0’, ‘P’ and ‘P0’ procedures.

<sup>#4</sup> We refer to positive (negative) polarisation as right- (left-) handed respectively.

reflection of the sign reversal of the forward-backward asymmetry in  $\cos \theta$ . Qualitatively similar results are obtained for up-type quarks, and for other values of  $y_c$ .

We illustrate the energy dependence of the  $\cos \theta$ - and  $\chi$ -distributions in Figs. 4a and 4b, respectively, for down-type quarks at fixed electron polarisation  $p = +1$ , with results at  $\sqrt{s} = 35, 60, 91$  and  $200$  GeV, corresponding to  $e^+e^-$  annihilation at the PETRA, TRISTAN, SLC/LEP and LEP2 collider energies. The variation with energy is due to the varying relative contribution of  $\gamma$  and  $Z^0$  exchange in the  $e^+e^-$  annihilation process. Results are also shown for a possible high-energy collider operating with polarised electrons at  $\sqrt{s} = 500$  GeV and 2 TeV. If such a facility could be operated at lower energies, where, apart from  $\sqrt{s} = 91$  GeV (SLC), polarised beams were not previously available, measurements in the same experiment of the distributions shown in Figs. 4(a,b) would provide a significant consistency check of the Standard Model.

#### 4. Polar- and Azimuthal-Angle Asymmetries

By analogy with the *left-right forward-backward asymmetry* of the polar-angle distribution:

$$\begin{aligned} \tilde{A}_{\text{FB}}(|p|)|_{\cos \theta} & \\ \equiv & \frac{\int_0^1 \frac{d\sigma^{\text{L}}}{d\cos \theta} d\cos \theta - \int_{-1}^0 \frac{d\sigma^{\text{L}}}{d\cos \theta} d\cos \theta - \left( \int_0^1 \frac{d\sigma^{\text{R}}}{d\cos \theta} d\cos \theta - \int_{-1}^0 \frac{d\sigma^{\text{R}}}{d\cos \theta} d\cos \theta \right)}{\int_0^1 \frac{d\sigma^{\text{L}}}{d\cos \theta} d\cos \theta + \int_{-1}^0 \frac{d\sigma^{\text{L}}}{d\cos \theta} d\cos \theta + \int_0^1 \frac{d\sigma^{\text{R}}}{d\cos \theta} d\cos \theta + \int_{-1}^0 \frac{d\sigma^{\text{R}}}{d\cos \theta} d\cos \theta}, \end{aligned} \quad (14)$$

we define a corresponding asymmetry of the azimuthal-angle distribution:

$$\tilde{A}(|p|)|_{\chi} \equiv \frac{\int_{\frac{\pi}{2}}^{\pi} \frac{d\sigma^{\text{L}}}{d\chi} d\chi - \int_0^{\frac{\pi}{2}} \frac{d\sigma^{\text{L}}}{d\chi} d\chi - \left( \int_{\frac{\pi}{2}}^{\pi} \frac{d\sigma^{\text{R}}}{d\chi} d\chi - \int_0^{\frac{\pi}{2}} \frac{d\sigma^{\text{R}}}{d\chi} d\chi \right)}{\int_{\frac{\pi}{2}}^{\pi} \frac{d\sigma^{\text{L}}}{d\chi} d\chi + \int_0^{\frac{\pi}{2}} \frac{d\sigma^{\text{L}}}{d\chi} d\chi + \int_{\frac{\pi}{2}}^{\pi} \frac{d\sigma^{\text{R}}}{d\chi} d\chi + \int_0^{\frac{\pi}{2}} \frac{d\sigma^{\text{R}}}{d\chi} d\chi}, \quad (15)$$

where  $\sigma^{\text{L,R}} = \sigma(\mp|p|)$  is the  $e^+e^- \rightarrow q\bar{q}g$  cross-section for a left- (L) or right- (R) handed electron beam of polarisation magnitude  $|p|$ .

For the case of  $e^+e^-$  annihilation at the  $Z^0$  resonance using electrons of longitudinal polarisation  $p$  and unpolarised positrons, as at SLC, eqs. (4) and (5) reduce to the simple forms

$$\begin{aligned} h_f^{(1)}(M_Z^2) &= |f(M_Z^2)|^2[(v^2 + a^2) - 2vap](v_f^2 + a_f^2), \\ h_f^{(2)}(M_Z^2) &= |f(M_Z^2)|^2[-(v^2 + a^2)p + 2va]2v_fa_f, \end{aligned} \quad (16)$$

and hence

$$\begin{aligned}\tilde{A}_{\text{FB}}(|p|)|_{\cos\theta} &= \frac{3}{4} |p| \frac{\hat{\sigma}_{\text{P}}}{\hat{\sigma}_{\text{U}} + \hat{\sigma}_{\text{L}}} A_f, \\ \tilde{A}(|p|)|_{\chi} &= \frac{3}{\sqrt{2}} |p| \frac{\hat{\sigma}_{\text{A}}}{\hat{\sigma}_{\text{U}} + \hat{\sigma}_{\text{L}}} A_f,\end{aligned}\tag{17}$$

where we use the common notation  $A_f \equiv 2v_f a_f / (v_f^2 + a_f^2)$ . Whereas both asymmetries are directly proportional to the beam polarisation  $|p|$  and the electroweak coupling  $A_f$ , the  $\cos\theta$  asymmetry is proportional to the helicity cross-section  $\hat{\sigma}_{\text{P}}$ , and the  $\chi$  asymmetry to the helicity cross-section  $\hat{\sigma}_{\text{A}}$ . Since the electroweak factor  $A_f$  is predicted to a high degree of accuracy by the Standard Model, and, in the case of b and c quarks, has been measured using predominantly  $q\bar{q}$  final states at SLC and LEP [6], measurement of these asymmetries in  $q\bar{q}g$  events at SLC/SLD would allow one to probe  $\hat{\sigma}_{\text{P}}$  and  $\hat{\sigma}_{\text{A}}$ , which have yet to be investigated experimentally. Furthermore, the ratio of the asymmetries is independent of both polarisation and electroweak couplings and depends only on the ratio of  $\hat{\sigma}_{\text{P}}$  and  $\hat{\sigma}_{\text{A}}$ :

$$\frac{\tilde{A}_{\text{FB}}(|p|)|_{\cos\theta}}{\tilde{A}(|p|)|_{\chi}} = \frac{\sqrt{2}}{4} \frac{\hat{\sigma}_{\text{P}}}{\hat{\sigma}_{\text{A}}}.\tag{18}$$

As a consequence of there being, up to  $\mathcal{O}(\alpha_s^2)$  in massless perturbative QCD, only the six independent helicity cross-sections given in eq. (3), the relations (17) and (18) are valid up to the same order.

We have calculated at  $\mathcal{O}(\alpha_s)$  the ratios  $\hat{\sigma}_{\text{P}}/(\hat{\sigma}_{\text{U}} + \hat{\sigma}_{\text{L}})$  and  $\hat{\sigma}_{\text{A}}/(\hat{\sigma}_{\text{U}} + \hat{\sigma}_{\text{L}})$  and show in Fig. 5a their dependence on  $y_c$ ; the dependence is weak. For completeness we also show  $\hat{\sigma}_{\text{T}}/(\hat{\sigma}_{\text{U}} + \hat{\sigma}_{\text{L}})$  and  $\hat{\sigma}_{\text{I}}/(\hat{\sigma}_{\text{U}} + \hat{\sigma}_{\text{L}})$ . It would be worthwhile to investigate the size of higher-order perturbative QCD contributions by evaluating these ratios at  $\mathcal{O}(\alpha_s^2)$ ; this should, in principle, be possible using the matrix elements described in Ref. [14]. It should then also be possible to estimate  $\mathcal{O}(\alpha_s^3)$  contributions using *ad hoc* theoretical procedures [15]. It would also be worthwhile to investigate quark mass effects; this could be done at  $\mathcal{O}(\alpha_s)$  using an available calculation [16], and at  $\mathcal{O}(\alpha_s^2)$  when the corresponding matrix elements [17] become available.

If higher-order perturbative contributions and mass corrections were under control, one could confront the theoretical predictions with experimental measurements. Significant deviations of the data from the predictions for the asymmetries, eqs. (17), would

indicate anomalous parity-violating contributions to the process  $e^+e^- \rightarrow q\bar{q}g$ , and the ratio of asymmetries, eq. (18), being at lowest order independent of the electroweak coupling factor  $A_f$ , would help to unravel the dynamical origin of any effect. For example, an *ad hoc* modification of strong interactions including an explicitly parity-violating quark-gluon coupling proportional to  $(1 - \epsilon\gamma_5)$  leads to  $O(\epsilon)$  corrections to  $\hat{\sigma}_i$  for  $i = P$  and  $A$ , as well as  $i = U, L, T$  and  $I$ ; it also leads to an additional small term proportional to  $\epsilon \sin \theta \sin \chi$  [18].

## 5. Moments of the Angular Distributions

The potential sensitivity of the six independent helicity cross-sections  $\sigma_i$  to strong parity-violating effects<sup>#5</sup> has led us to consider a generalised method for extracting them from data. We define moments of the cross-section (3) in terms of powers of  $\cos \theta$  and  $\cos \chi$ :

$$\Sigma_{mn} \equiv \int_{-1}^1 d(\cos \theta) \cos^m \theta \int_0^{2\pi} d\chi \cos^n \chi \int_{y_c} dx \int d\bar{x} \frac{d^4\sigma}{d(\cos \theta)d\chi dx d\bar{x}}. \quad (19)$$

The lowest-rank moments are given in Table 1, where the  $\hat{\sigma}_i$  are defined by eq. (11). It should be noted that  $\Sigma_{00}$  corresponds to the total integrated cross-section for 3-jet production, and that  $\Sigma_{01}$  and  $\Sigma_{10}$  are closely related to the asymmetries defined by eqs. (14) and (15). It then follows trivially that each  $\hat{\sigma}_i$  could be obtained from the measured moments:

$$\begin{aligned} \hat{\sigma}_U &= (5\Sigma_{20} - \Sigma_{00})/h_f^{(1)}(s), & \hat{\sigma}_L &= (2\Sigma_{00} - 5\Sigma_{20})/h_f^{(1)}(s), \\ \hat{\sigma}_T &= (4\Sigma_{02} - 2\Sigma_{00})/h_f^{(1)}(s), & \hat{\sigma}_I &= \left( \frac{16\sqrt{2}}{3\pi} \Sigma_{11} \right) / h_f^{(1)}(s), \\ \hat{\sigma}_A &= \left( \frac{-4\sqrt{2}}{3\pi} \Sigma_{01} \right) / h_f^{(2)}(s), & \hat{\sigma}_P &= 2\Sigma_{10}/h_f^{(2)}(s), \end{aligned} \quad (20)$$

where the electroweak parameters entering via eqs. (4) and (5) could be taken from the Standard Model, or from measured values based predominantly on 2-jet final states.

---

<sup>#5</sup> More generally the  $\sigma_i$  are, of course, sensitive to the strong dynamics. For example, in a scalar-gluon theory at  $y_c = 0.02$ ,  $\hat{\sigma}_A/(\hat{\sigma}_U + \hat{\sigma}_L)$  and  $\hat{\sigma}_P/(\hat{\sigma}_U + \hat{\sigma}_L)$  differ by factors of  $-1.5$  and  $0.12$ , respectively, relative to QCD.



## 6. Inclusive Cross-Sections

All of the preceding discussions have been based on the assumption that the parton-type originator of jets is known, *i.e.* that in  $e^+e^- \rightarrow 3\text{-jet}$  events one can identify which jet originated from the quark, antiquark and gluon. The definition of  $\cos\theta$  requires that the quark jet be known, whereas the definition of  $\chi$  requires that both the quark jet and a second jet origin be known. It is difficult from an experimental point-of-view to make such exclusive identification for jets of hadrons measured in a detector. Quark and antiquark jets have been identified in predominantly 2-jet events in  $e^+e^-$  annihilation (see *e.g.* [7]), where typically only one jet per event is tagged, with low efficiency. Identification of both quark and antiquark jets in  $e^+e^- \rightarrow q\bar{q}g$  events is *a priori* more difficult due to the greater hadronic activity, and the overall efficiency is very low since it is proportional to the square of the single-jet tagging efficiency.

It is therefore useful to consider more inclusive quantities. Two possibilities are: (1) *Semi-inclusive*: the quark jet is assumed to be identified, and the *least energetic* jet in the event is taken to be the gluon and is used to define the angle  $\chi$  (eq. (1)). (2) *Fully-inclusive*: the jets are labelled only in terms of their energies,  $x_3 \leq x_2 \leq x_1$ ; the polar angle  $\theta$  is then defined by the angle of the fastest jet w.r.t. the electron beam direction<sup>#6</sup>, and the azimuthal angle  $\chi$  can be defined analogously to eq. (1) as:

$$\cos\chi = \frac{\vec{1} \times \vec{3}}{|\vec{1} \times \vec{3}|} \cdot \frac{\vec{1} \times \vec{e}^-}{|\vec{1} \times \vec{e}^-|} \quad (21)$$

In both cases a similar moments analysis to that defined in Section 5 can be applied, with relations between the corresponding helicity cross-sections and the lowest-rank moments as given in Table 1.

For the semi-inclusive case we have calculated the  $\hat{\sigma}_i$  at  $O(\alpha_s)$  and show the ratios  $\hat{\sigma}_T/(\hat{\sigma}_U + \hat{\sigma}_L)$ ,  $\hat{\sigma}_I/(\hat{\sigma}_U + \hat{\sigma}_L)$ ,  $\hat{\sigma}_P/(\hat{\sigma}_U + \hat{\sigma}_L)$  and  $\hat{\sigma}_A/(\hat{\sigma}_U + \hat{\sigma}_L)$  in Fig. 5b. Whereas  $\hat{\sigma}_P$  and  $\hat{\sigma}_T$  are unchanged relative to the exclusive case,  $\hat{\sigma}_I$  and  $\hat{\sigma}_A$ , which multiply terms proportional to  $\cos\chi$  in eq. (3), are smaller in magnitude because of the sometimes incorrect gluon-jet identification. Though this implies that the parity-violating asymmetry  $\tilde{A}(|p|)|_\chi$  in eq. (17) is smaller by a ( $y_c$ -dependent) factor of order 2, it will in fact

---

<sup>#6</sup> To  $O(\alpha_s)$  this is equivalent to the angle of the thrust axis [19] w.r.t. the electron direction.

be easier to access experimentally because the semi-inclusive case requires only one of the quark- and antiquark-jets to be identified explicitly.

In the fully-inclusive case the terms  $\sigma_A$  and  $\sigma_P$ , which are odd under interchange of quark and antiquark jets, cancel out; writing the cross-section in terms of thrust [19] one obtains at  $O(\alpha_s)$ :

$$2\pi \frac{d^3\sigma}{d(\cos\theta)d\chi dT} = \frac{3}{8}(1 + \cos^2\theta) \frac{d\sigma_U}{dT} + \frac{3}{4}\sin^2\theta \frac{d\sigma_L}{dT} \\ + \frac{3}{4}\sin^2\theta \cos 2\chi \frac{d\sigma_T}{dT} + \frac{3}{2\sqrt{2}}\sin 2\theta \cos \chi \frac{d\sigma_I}{dT}, \quad (22)$$

where expressions for  $d\sigma_i/dT$  can be found in ref. [8]<sup>#7</sup>. Using the notation

$$\tilde{\sigma}_i \equiv \int_{y_c} \frac{d\sigma_i}{dT} dT, \quad i = U, L, T, I,$$

we have calculated the  $\tilde{\sigma}_i$  at  $O(\alpha_s)$  and show the ratios  $\tilde{\sigma}_T/(\tilde{\sigma}_U + \tilde{\sigma}_L)$  and  $\tilde{\sigma}_I/(\tilde{\sigma}_U + \tilde{\sigma}_L)$  in Fig. 5c. Their magnitudes and dependences on  $y_c$  differ relative to the exclusive and semi-inclusive cases due to the redefinition of  $\theta$  and  $\chi$ . Distributions of  $\cos\theta$  and  $\chi$  in this case have already been measured and found to be in agreement with  $O(\alpha_s)$  QCD calculations [20], [21].

Another fully-inclusive observable is the polar-angle  $\bar{\theta}$  of the normal to the event plane with respect to the beam direction. The differential cross-section  $d\sigma/d(\cos\bar{\theta})$  has been calculated at  $O(\alpha_s^2)$  in massless perturbative QCD [22], and has been measured at  $\sqrt{s} \simeq 35$  GeV [20] and  $\sqrt{s} = 91$  GeV [21]. The effects of final-state interactions can induce a term linear in  $\cos\bar{\theta}$  whose sign and magnitude depend on the electron beam polarisation [23]; experimental limits on such a term have been set using hadronic  $Z^0$  decays [24].

---

<sup>#7</sup> Note that  $d\sigma_I/dT$  has opposite sign as compared with ref. [8], since the angle  $\chi$  defined by eq. (21) is complementary to that of ref. [8],  $\chi_{\text{eq. (21)}} = \pi - \chi_{\text{ref. [8]}}$ .

## 7. Conclusions

We have presented the orientation of  $e^+e^- \rightarrow q\bar{q}g$  events in terms of the polar- ( $\theta$ ) and azimuthal- ( $\chi$ ) angle distributions. These distributions have been calculated at  $O(\alpha_s)$  in perturbative QCD for massless quarks and their dependence on longitudinal electron-beam polarisation and centre-of-mass energy has been illustrated. We have considered the left-right forward-backward asymmetry of the  $\cos\theta$  distribution and have defined a corresponding asymmetry of the  $\chi$  distribution. Parity-violating 3-jet observables of this kind represent a new search-ground for anomalous contributions and have yet to be explored experimentally.

For the case of  $e^+e^-$  annihilation at the  $Z^0$  resonance using longitudinally-polarised electrons, the  $\cos\theta$  asymmetry is proportional to the QCD helicity cross-section  $\hat{\sigma}_P$ , and the  $\chi$  asymmetry to the helicity cross-section  $\hat{\sigma}_A$ , which have not yet been measured; this should be possible, with a high-statistics data sample, using the highly-polarised electron beam at SLC/SLD. To lowest electroweak order the ratio of these asymmetries is independent of electroweak couplings and the beam polarisation. These results are valid up to  $O(\alpha_s^2)$  in QCD perturbation theory. We have calculated  $\hat{\sigma}_P$  and  $\hat{\sigma}_A$  at  $O(\alpha_s)$  and find their dependence on the jet resolution parameter  $y_c$  to be weak. It would be worthwhile to calculate higher-order perturbative QCD contributions, as well as quark mass effects, before making a detailed comparison of these predictions with data.

We have also defined moments of the cross-section in terms of powers of  $\cos\theta$  and  $\cos\chi$ , which allow the six independent helicity contributions  $\hat{\sigma}_U, \hat{\sigma}_L, \hat{\sigma}_T, \hat{\sigma}_I, \hat{\sigma}_P$  and  $\hat{\sigma}_A$  to be determined from data. Even the extraction of  $\hat{\sigma}_U, \hat{\sigma}_L, \hat{\sigma}_T$  and  $\hat{\sigma}_I$ , which does not require quark and antiquark jet identification, represents a detailed test of QCD.

This research has been supported by U.S. Department of Energy Cooperative Agreement DE-FC02-94ER40818 and by the Research Council of Norway. We thank Lance Dixon and Tom Rizzo for helpful discussions.

## References

- [1] TASSO Collab., R. Brandelik *et al.*, Phys. Lett. **86B** (1979) 243.  
Mark J Collab., D.P. Barber *et al.*, Phys. Rev. Lett. **43** (1979) 830.  
PLUTO Collab., Ch. Berger *et al.*, Phys. Lett. **86B** (1979) 418.  
JADE Collab., W. Bartel *et al.*, Phys. Lett. **91B** (1980) 142.
- [2] H. Fritzsch, M. Gell-Mann and H. Leutwyler, Phys. Lett. **47B** (1973) 365;  
D.J. Gross and F. Wilczek, Phys. Rev. Lett. **30** (1973) 1343;  
H.D. Politzer, Phys. Rev. Lett. **30** (1973) 1346;  
S. Weinberg, Phys. Rev. Lett. **31** (1973) 494.
- [3] For a review see S.L. Wu, Phys. Rep. **107** (1984) 59.
- [4] See, *e.g.*, G. Altarelli *et al.*, in Physics at LEP, CERN 86-02 (1986), eds. J. Ellis and R. Peccei, p. 1.
- [5] See, *e.g.*, T. Kamae, in Proc. XXIV International Conference on High Energy Physics, Munich, August 4–10, 1988 (eds. R. Kotthaus and J.H. Kühn, Springer Verlag, 1989) p. 156.
- [6] A. Blondel, to appear in Proc. XXVIII International Conference on High Energy Physics, Warsaw, Poland, July 25–31 1996.
- [7] SLD Collab., K. Abe *et al.*, Phys. Rev. Lett. **74** (1995) 2890; *ibid* **74** (1995) 2895; *ibid* **75** (1995) 3609.
- [8] H.A. Olsen, P. Osland, I. Øverbø, Nucl. Phys. **B171** (1980) 209.
- [9] P. Nason, B.R. Webber, Nucl. Phys. **B421** (1994) 473; Erratum: *ibid* **B480** (1996) 755.
- [10] J.G. Körner, G.A. Schuler, Z. Phys. **C26** (1985) 559.
- [11] E. Laermann, K.H. Streng, P.M. Zerwas, Z. Phys. **C3** (1980) 289; Erratum: Z. Phys. **C52** (1991) 352.
- [12] S. Bethke *et al.*, Nucl. Phys. **B370** (1992) 310.
- [13] SLD Collab., K. Abe *et al.*, SLAC-PUB-7291 (1996); subm. to Phys. Rev. Lett.
- [14] S. Catani, M. Seymour, CERN-TH-96-029 (1996).
- [15] M.A. Samuel, G. Li, E. Steinfelds, Phys. Rev. **D48** (1993) 869;  
A.L. Kataev, V.V. Starshenko, Mod. Phys. Lett. **A10** (1995) 235.
- [16] J.B. Stav, H.A. Olsen, Phys. Rev. **D50** (1994) 6775.
- [17] A. Ballestrero, E. Maina, S. Moretti, Phys. Lett. **B294** (1992) 425;  
M. Bilenkii, G. Rodrigo, A. Santamaria, Nucl. Phys. **B439** (1995) 505;  
A. Brandenburg, private communications.
- [18] O.M. Øgreid, Cand. Scient. Thesis, University of Bergen, October 1993 (unpublished).

- [19] E. Farhi, Phys. Rev. Lett. **39** (1977) 1587.
- [20] TASSO Collab., W. Braunschweig *et al.*, Z. Phys. **C47** (1990) 181.
- [21] L3 Collab., B. Adeva *et al.*, Phys. Lett. **B263** (1991) 551.  
DELPHI Collab., P. Abreu *et al.*, Phys. Lett. **B274** (1992) 498.  
SLD Collab., K. Abe *et al.*, SLAC-PUB-7099 (1996); to appear in Phys. Rev. D.
- [22] J.G. Körner, G.A. Schuler, F. Barreiro, Phys. Lett. **B188** (1987) 272.
- [23] A. Brandenburg, L. Dixon, Y. Shadmi, Phys. Rev. **D53** (1996) 1264.
- [24] SLD Collab., K. Abe *et al.*, Phys. Rev. Lett. **75** (1995) 4173.

Table 1: Cross-section moments  $\Sigma_{mn}$

	$n = 0$	$n = 1$	$n = 2$
$m = 0$	$(\hat{\sigma}_{\text{U}} + \hat{\sigma}_{\text{L}}) h_f^{(1)}(s)$	$-\frac{3\pi}{4\sqrt{2}} \hat{\sigma}_{\text{A}} h_f^{(2)}(s)$	$(\frac{1}{2} \hat{\sigma}_{\text{U}} + \frac{1}{2} \hat{\sigma}_{\text{L}} + \frac{1}{4} \hat{\sigma}_{\text{T}}) h_f^{(1)}(s)$
$m = 1$	$\frac{1}{2} \hat{\sigma}_{\text{P}} h_f^{(2)}(s)$	$\frac{3\pi}{16\sqrt{2}} \hat{\sigma}_{\text{I}} h_f^{(1)}(s)$	$\frac{1}{4} \hat{\sigma}_{\text{P}} h_f^{(2)}(s)$
$m = 2$	$(\frac{2}{5} \hat{\sigma}_{\text{U}} + \frac{1}{5} \hat{\sigma}_{\text{L}}) h_f^{(1)}(s)$	$-\frac{3\pi}{16\sqrt{2}} \hat{\sigma}_{\text{A}} h_f^{(2)}(s)$	$(\frac{1}{5} \hat{\sigma}_{\text{U}} + \frac{1}{10} \hat{\sigma}_{\text{L}} + \frac{1}{20} \hat{\sigma}_{\text{T}}) h_f^{(1)}(s)$

## Figure Captions

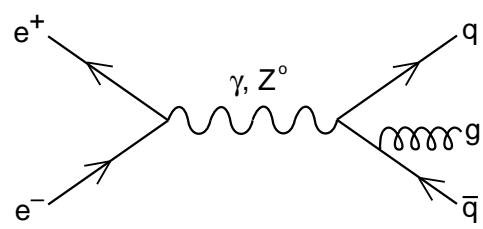
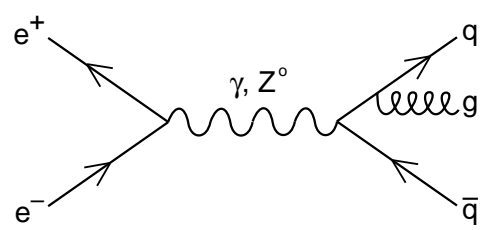
Fig. 1: Tree-level Feynman diagrams for three-jet production in  $e^+e^-$  annihilation.

Fig. 2: Definition of the angles  $\theta$  and  $\chi$ .

Fig. 3: Angular orientation of the event plane for down-type quarks and  $y_c = 0.02$ . Distribution of (a)  $\cos\theta$  and (b)  $\chi$  at  $\sqrt{s} = M_Z$ , for 5 values of  $p$ .

Fig. 4: Angular orientation of the event plane for down-type quarks and  $y_c = 0.02$ . Distribution of (a)  $\cos\theta$  and (b)  $\chi$  for  $p = +1$  at 6 values of  $\sqrt{s}$ .

Fig. 5: Helicity cross-section ratios (see text) as functions of  $y_c$ ; (a) exclusive, (b) semi-inclusive and (c) fully-inclusive cases. For the sake of clarity, the ratios are multiplied by a factor of 5 where indicated.

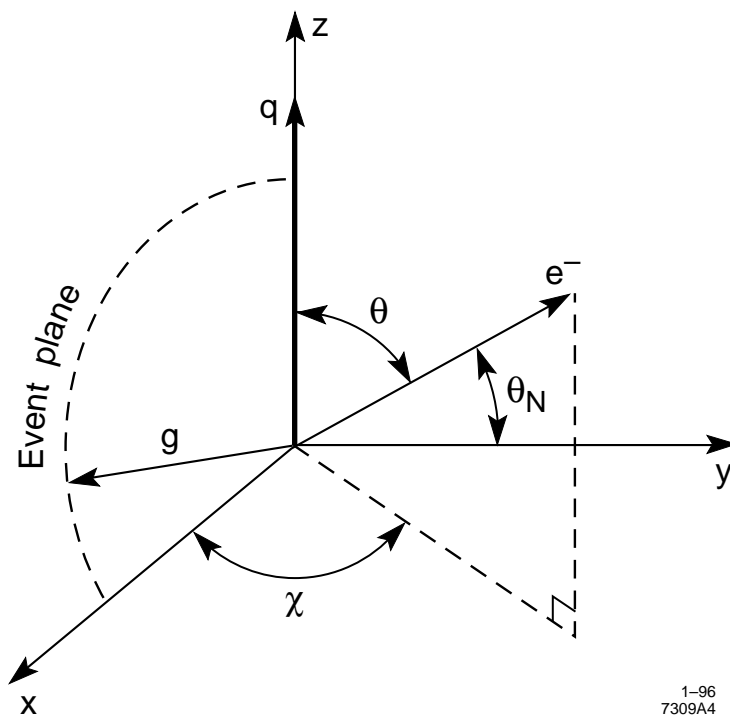


12-92

7309A1

Fig. 1





1-96  
7309A4

Fig. 2

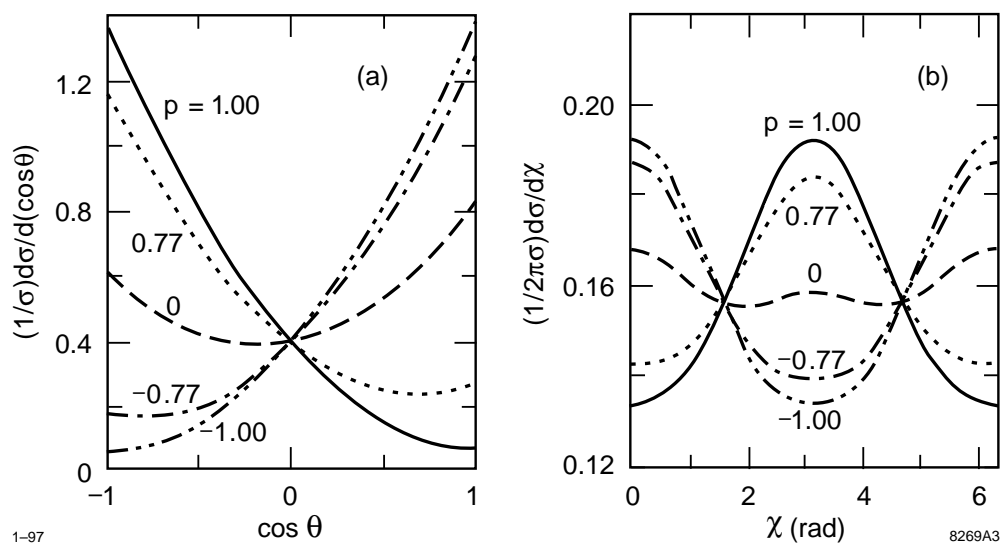


Fig. 3

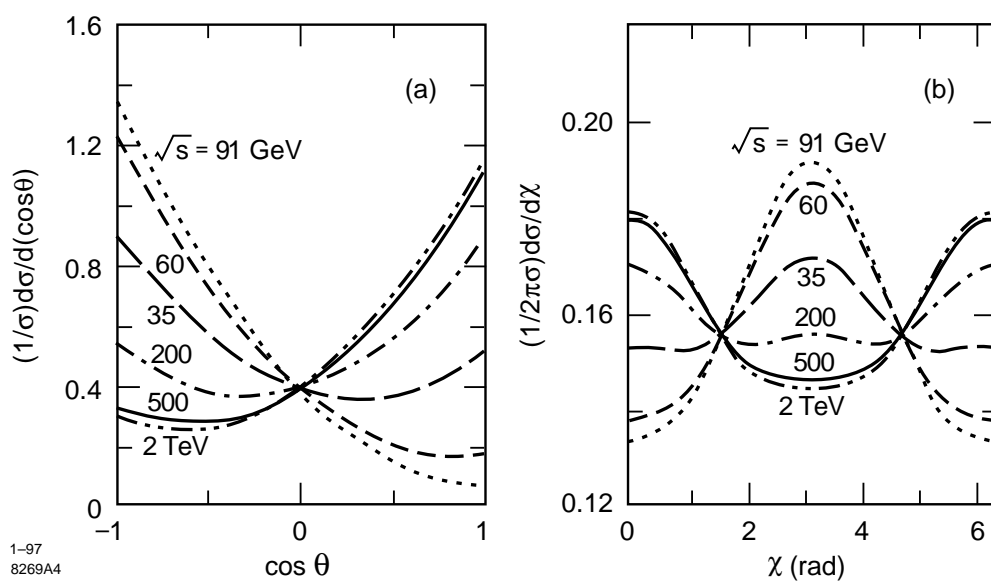


Fig. 4

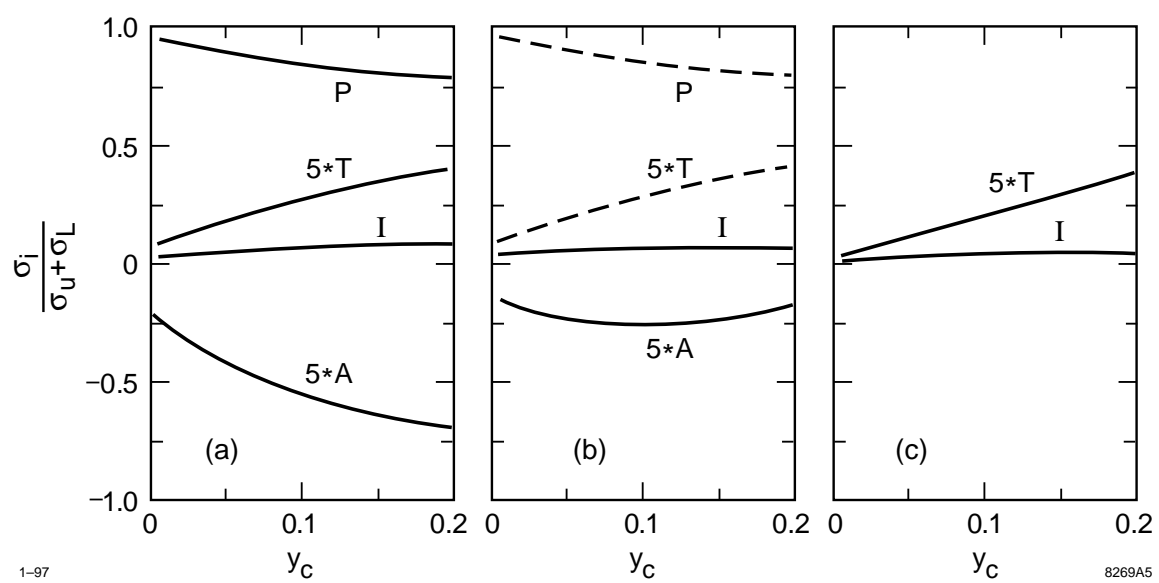


Fig. 5